Nanoscale

COMMUNICATION

Cite this: *Nanoscale*, 2024, **16**, 6449

Received 15th October 2023,
Accepted 22nd February 2024

DOI: 10.1039/d3nr05205b

rsc.li/nanoscale

Uncovering thermally activated purple-to-blue luminescence in Co-modified MgAl-layered double hydroxide†

Bianca R. Gevers, *[a,b] Emil Roduner, [c,d] Andreas Leuteritz[b] and Frederick J. W. J. Labuschagné[a]

Thermally activated blue-to-purple luminescence of Co-modified nano-sandrose MgAl-layered double hydroxides (LDHs) is concentration dependent, occurring only for MgCoAl-LDH with a molar metal cation concentration of 15% Co. Temperature sweep luminescence spectroscopy between 83 K and 298 K shows that the luminescence is strongest at room temperature, increasing with an activation energy of 1 kJ mol^{-1} between these temperatures. The luminescence occurs in a broad, but fine-structured band below the conduction band (CB) edge at 3.0 eV after excitation at 5.0 eV.

Thermally-activated luminescence is a rare phenomenon[1] taken advantage of for interesting applications such as light-emitting diodes (LEDs) specifically of organic type (OLED),[2,3] scintillators[4] and thermal sensing.[5] The thermal activation stands in contrast to common luminescence behaviour, where the intensity of luminescence decreases with an increase in temperature due to increased lattice vibration amplitudes, which allow excited electrons to non-radiatively relax to the ground state through a release of heat.[6] Inorganic, nano-sized materials that have shown this kind of behaviour are, for example, perovskites.[2,4,5,7] For LDHs, this kind of behaviour has not been observed previously.

LDHs are layered materials with the formula $[M^{II}_{1-x}M^{III}_{x}(OH)_2][X_{x/q}{}^{q-}\cdot nH_2O]$, where M^{II} and M^{III} are divalent and trivalent cations that combine with the interlayer anion $X_{x/q}{}^{q-}$ (q = charge, x = molar fraction of trivalent to total cations in the layer) to create a layered structure similar to brucite.[8,9] LDHs house a complicated set of bonds—ionic, ionic/dipolar, dipolar, hydrogen bonds and van der Waals interactions—which stabilise the layered structure and give it interesting and complex fundamental properties.[10]

As a result of these interesting properties and the ability to easily modify their composition and morphology through variation of the synthesis parameters,[10,11] LDHs (and especially transition-metal modified LDHs) have gained prominence in studies concerning their use in advanced applications such photocatalysis,[12] electrolysis,[13,14] solar cells,[15,16] supercapacitors[17–19] and sensors.[20,21] Recently, there has been particular interest in their application as LEDs.[22–26] However, luminescence efficiency is still being optimised.

In this communication we report the thermally activated luminescence of bulk, nano-sandrose MgCoAl-LDH, leading to significant increases in luminescence intensity in the purple-to-blue-light region. Its concentration dependence is explored through comparison of the optical properties of MgAl-LDH, MgCoAl-1, MgCoAl-2, MgCoAl-9, MgCoAl-15, MgCoAl-34, MgCoAl-52, MgCoAl-69 and CoAl-LDH (MgAl-LDHs modified with 1 mol% to 100 mol% of Co through replacement of Mg in the structure).

The LDHs were prepared using co-precipitation,[27] forming crystalline impurity-free, nano-sandrose (see Fig. S3†) structures approximately 200 nm in diameter of rhombohedral polytype (3R) in the $R\bar{3}m$ space group[9,28] with the characteristic (003), (006), (009), (015), (019), (110) and (113) reflections and expected shifts of reflections as a result of Co-replacement observable in the X-ray diffraction scans (Fig. S1†). The ESI† describes the preparation method used and shows material data (crystal structures, compositions and morphology) for the 9 materials in more detail.

Fig. 1(a) depicts the absorption spectra of the series of LDHs. With an increase in Co, the absorption strength increases significantly and is strongest for MgCoAl-52, MgCoAl-69 and CoAl-LDH. The region between 3.0 eV to 6.2 eV, is populated by oxygen-to-metal charge transfer transitions (O-2p → Mg-, Al-3s/p and Co-3d).[11] An increase in Co-content markedly increases the absorption strength, but is most domi-

[a]*Department of Chemical Engineering, University of Pretoria, 0002 Pretoria, South Africa. E-mail: bianca.gevers@tuks.co.za*
[b]*Leibniz-Institut für Polymerforschung Dresden e.V., Institute of Polymer Materials; Processing Technology, D-01069 Dresden, Germany*
[c]*Department of Chemistry, University of Pretoria, 0002 Pretoria, South Africa*
[d]*Institute of Physical Chemistry, Universität Stuttgart, Stuttgart D-70569, Germany*

†Electronic supplementary information (ESI) available: X-ray diffraction patterns, SEM images, compositional data, sample photographs, Tauc plot bandgap analysis and luminescence repeatability results. See DOI: **https://doi.org/10.1039/d3nr05205b**

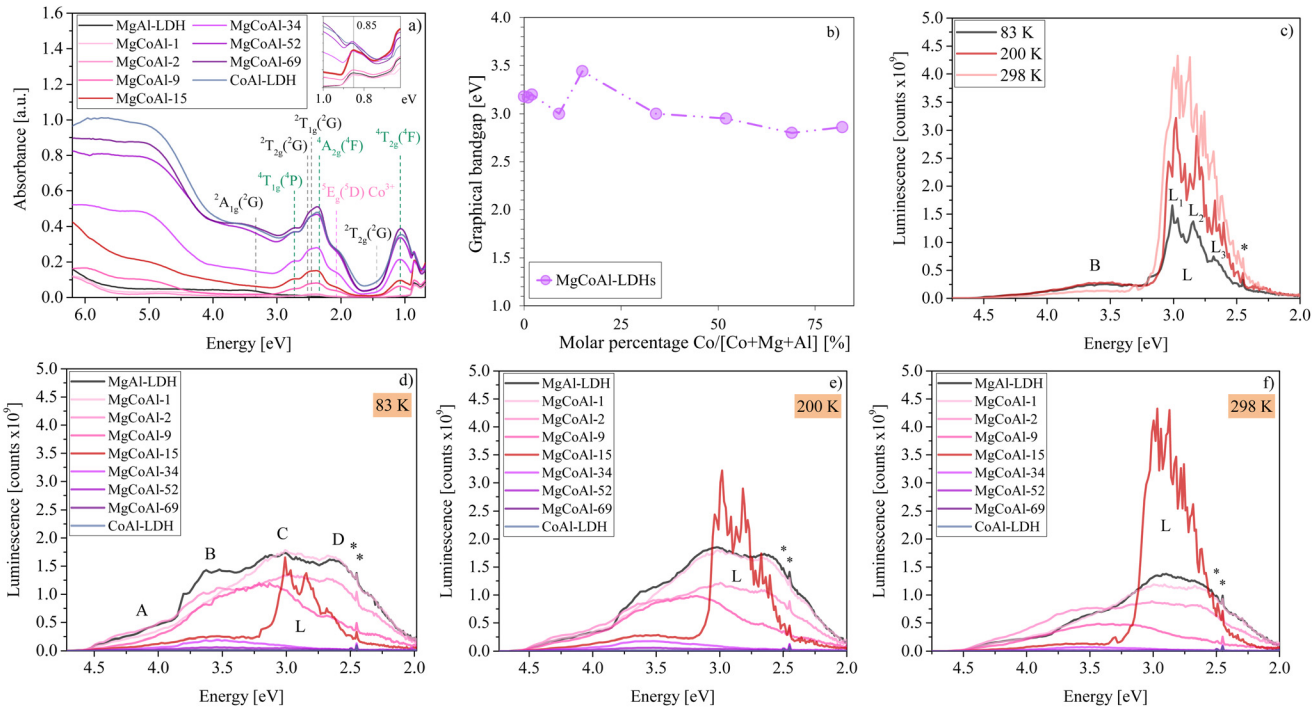

Fig. 1 (a) Diffuse-reflectance absorption spectra of MgCoAl-LDHs with Co-modifications between 0% (MgAl-LDH) and 100% (CoAl-LDH). The inset depicts the abrupt increase in absorption at 0.85 eV for MgCoAl-15. A change in absorption is only distinctly visible from MgCoAl-9. (b) Tauc plot (graphical) bandgaps of MgCoAl-LDHs with Co-modifications between 0% (MgAl-LDH) and 100% (CoAl-LDH) showing a deviation in bandgap trend for MgCoAl-15. (c) Comparison of temperature-dependent MgCoAl-15 luminescence spectra with subdivision of band L into L_1, L_2 and L_3. Luminescence spectra of MgCoAl-LDHs with Co-modifications between 0% (MgAl-LDH) and 100% (CoAl-LDH) at (d) 83 K, (e) 200 K and (f) 298 K subdivided into four bands (A, B, C and D[10]) showing the thermally activated luminescence of MgCoAl-15 in band L. λ_{ex} = 5.0 eV for all luminescence spectra. The luminescence depression of MgCoAl-52, MgCoAl-69 and CoAl-LDH is so significant, that their spectra overlap just above the baseline.

nant only from MgCoAl-15. This is expected to occur as a result of an increasing hybridisation of Co states in the CB.[11] In addition, the absorption spectra contain strong, narrow, overlapping absorption bands in the visible to near-infrared light region which can be ascribed approximately to spin-allowed (ν_1: $^4T_{1g}(^4F) \rightarrow {}^4T_{2g}(^4F)$, ν_2: $^4T_{1g}(^4F) \rightarrow {}^4A_{2g}(^4F)$, ν_3: $^4T_{1g}(^4F) \rightarrow {}^4T_{1g}(^4P)$, marked green), and to spin–forbidden (ν_4: $^4T_{1g}(^4F) \rightarrow {}^2T_{1g}(^2G)$ and ν_5: $^4T_{1g}(^4F) \rightarrow {}^2T_{2g}(^2G)$, marked black) d–d transitions originating from the excitation of the high-spin Co^{2+} ion in $3d^7$ configuration.[11,29] The band at 2.07 eV (marked with a pink line) can be ascribed to the spin-allowed excitation of low-spin Co^{3+} (favoured as a result of the low charge density) from $^1A_{1g}(^5D) \rightarrow {}^1T_{2g}(^1I)$.[11] The presence of this transition indicates that a fraction of the Co—which was desired to be included in the structure as Co^{2+}—is in fact present in the trivalent Co^{3+} form. This is supported by the compositional data shown in Fig. S4.† The latter indicates that the ratio of Co in the LDH structure is higher than expected, partially accommodated for by a reduction in Al-content. MgCoAl-15 contains 15 mol% of Co (Co/[Co + Mg + Al]) with a 22% replacement of Mg for Co. The amount of Co^{3+} present is estimated to be approximately 15% to 20% of the total Co content.

The size of the bandgap is crucial for the interpretation of luminescence mechanisms. An analysis of the graphical bandgaps (using the Tauc plot method, Fig. S6†) indicates, that the bandgap of the LDHs narrows slightly with increasing Co-content (see Fig. 1(b)) and is 3.44 eV for MgCoAl-15, based on an expected start of sufficient hybridisation of the Co states with those in the CB at this Co-content level.[11]

Notably, the bandgap value of MgCoAl-15 presents a deviation from the otherwise relatively uniform trend displayed in Fig. 1(b). The value of the bandgap of the other materials, hereby, overlaps with that of the thermally-activated luminescence band of MgCoAl-15 exactly, as can be observed on Fig. 1(c). The absorption spectra were obtained through measurement with an integrating sphere. It is thus believed, that this deviation from the bandgap trend is a result of the high luminescence in this region, counting towards reflection instead of absorption and skewing the absorption data recorded. Consequently, the true bandgap of MgCoAl-15 is believed to be 3.0 eV (matching the value of MgCoAl-9 and MgCoAl-34).

Once charges have been separated through photon absorption, excited electrons can relax to the ground state *via* non-radiative or radiative recombination with the hole in the valence band (VB) or they can diffuse to the surface where they may be captured. In the typical mechanism of luminescence, excited charges non-radiatively relax to the CB edge, from where they combine with a hole in the VB.[6] Fig. 1(d–f) shows

the luminescence spectra of MgAl-LDH modified (through molar replacement of Mg) with Co for percentages between 0 mol% (MgAl-LDH) and 100 mol% (CoAl-LDH). The luminescence spectra were obtained at three temperatures (83 K, 200 K and 298 K) and show a broad emission band with four sub-bands (A, B, C and D, similar to MgAl-LDH[10]) between 4.5 eV and 2.5 eV, and a shoulder extending to 2.0 eV.

Broad emission spectra are common for LDHs.[10,21,30,31] The broad emission spectra indicate, that the typical process of luminescence is not fully descriptive of that followed in the relaxation of excited charges in LDHs. In previous work,[10] the broad emission band of MgAl-LDH was subdivided into the same four bands (A, B, C, D, shown in Fig. 1(d)) with a shoulder extending to 2 eV. The bands were ascribed to radiative recombination from meta-stable CB states within an inhomogeneous CB above the band edge (bands A and B), radiative recombination from states just above the band edge and from the band edge (band C), and below-band-edge luminescence caused by effects of vibrational broadening, coordination defects, access to band-tail states, and exciton formation and its binding to defects/Al^{3+} islands in addition to the interlayer carbonate facilitating charge separation (band D and the shoulder).[10]

Fig. 1(d–f) show that, overall and excluding feature L, the emission is reduced across the four bands and within the region of the shoulder upon an increase in Co-concentration at all measurement temperatures. This is in line with frequent observations in LDHs, which show a reduction in luminescence intensity with increasing TM-content and is often argued to result in enhanced charge stabilisation.[32–34]

At Co concentrations of 1% and 2%, the spectra retain the same shape as the emission band for MgAl-LDH. From a Co content of 9%, the main emission slowly starts to shift from bands B, C and D to band B (general trend, excluding band L). Conversely, the absorption strength increases with an increase in Co content (Fig. 1(a)), opposing what could be expected: higher luminescence with higher absorption strength. Co is thus very effective at quenching luminescence (especially at high concentrations): with a 100 mol% Mg-for-Co replacement (CoAl-LDH), 99.3% of the luminescence of MgAl-LDH is quenched (based on the area under the MgAl-LDH spectrum between 5.0 eV and 2.0 eV).

However, very strikingly, the intermediate composition MgCoAl-15 displays a strong, relatively broad (roughly 0.5 eV FWHM (full width at half maximum)) emission band (L) with significant fine-structure (L_1, L_2 and L_3) and a peak luminescence (in L_1) at 3.01 eV, 2.98 eV and 2.97 eV at 83 K, 200 K and 298 K, respectively, in addition to band B visible in the other materials. The resolved fine structure with narrow lines shows that the origin of luminescence is a well-defined excitonic species with little to no variation of Coulomb energy.

The excitation energy (5.0 eV) falls within the highest intensity absorption band (see Fig. 2(a)), far above the band edge of MgCoAl-15 (3.0 eV). The luminescence of band B thus has an energy exceeding the bandgap, while the luminescence energy of band L matches the bandgap approximately at highest intensity. Since the luminescence of band B occurs with energies exceeding the bandgap, it suggests that a meta-stable band exists within the CB which allows this recombination behaviour.[10] At 298 K, the minimum of this meta-stable band sits approximately 0.55 eV above the CB edge (E_B on Fig. 2(b)). This process creates low intensity luminescence (6% of the total luminescence at 298 K), indicating that only a small fraction of excited charges relaxes through this mechanism. For all doping levels but MgCoAl-15, the lowering intensity of this band indicates that a large number of the excited charges have decayed non-radiatively.

As evidenced through Fig. 1(c–f), the sharp band L remains similar in width but becomes less defined and more intense with an increase in temperature, displaying thermally activated luminescence in the purple-to-blue region of the visible light spectrum. The temperature-dependence of the thermally activated luminescence suggests that an activation energy is required to be overcome. Assuming that it is the result of two competing processes, this activation energy was calculated based on the Arrhenius equation

$$k = A\, e^{-E_A/RT}$$

using the area under band L between 3.3 eV and 2 eV as k. This yields an activation energy of 707 J mol^{-1} between 83 K and 200 K, 2225 J mol^{-1} between 200 K and 298 K, and 994 J mol^{-1} between 83 K and 298 K. The activation energy is thus higher at 200 K than at 298 K or 83 K. This energy is indicated as E_A in Fig. 2(b).

In total, band L represents 94% of the total luminescence of MgCoAl-15 (at 298 K). Thus, only for MgCoAl-15, a new, efficient, thermally-activated recombination channel is opened, allowing excited charges to non-radiatively relax to the CB edge from where they recombine with a hole in the VB, leading to the formation of triple-band L. The thermally activated luminescence is not observed at any other Co-concentration and is reproducible (see Fig. S7†), although with variation in intensity.

Since band L only occurs reproducibly in a narrow Co-concentration range around 15 mol%, we propose that a sort of Co dimer is involved in the recombination mechanism, while isolated Co ions and clusters of multiple interacting Co ions likely do not contribute to this effect. Thus, in all materials but MgCoAl-15, Co acts as a trap for excited electrons and induces non-radiative recombination.

Luminescence properties of LDHs have rarely been investigated in depth in the past, leading to a large deficit in fundamental understanding of the broader optical properties of these materials, especially pertaining to recombination mechanisms. In the following paragraphs we wish to explore some explanations for the behaviour observed and also delve into the potential causes of the triple-band structure of the thermally activated luminescence.

Fig. 2(c) depicts two scenarios of ion-replacement in a perfectly ordered 2 : 1 MgAl-LDH lattice. In scenario 1, Al^{3+} is replaced by Co^{3+}. In scenario 2, Mg^{2+} is replaced by Co^{2+}. The

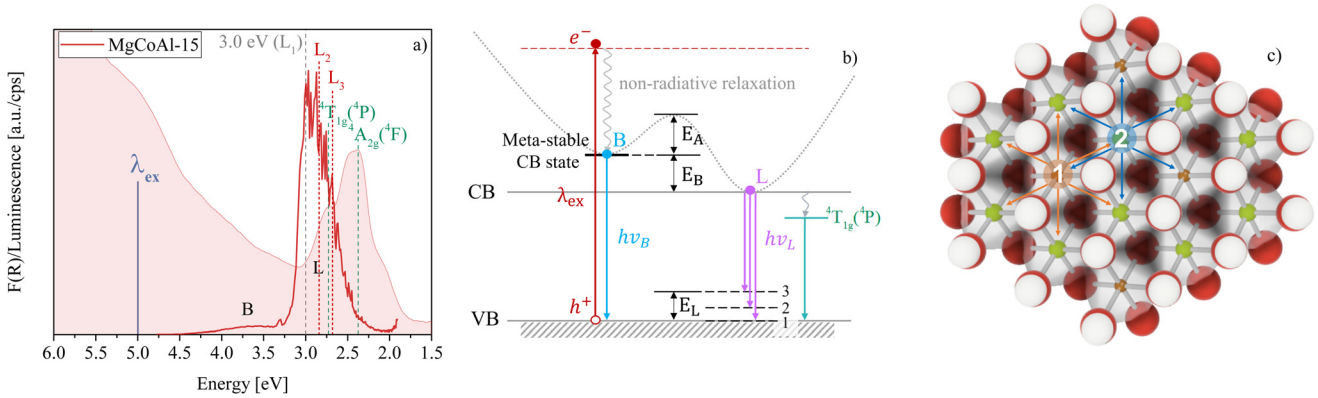

Fig. 2 (a) Comparison of the absorption and luminescence spectrum of MgCoAl-15 at 298 K. The position of the two spin-allowed d–d transitions $^4T_{1g}(^4P)$ and $^4A_{2g}(^4F)$ is indicated in green, while the position of the bandgap (3.0 eV overlapping with L_1) is depicted in grey and the positions of L_2 and L_3 are depicted in red. λ_{ex} = 5.0 eV. (b) Depiction of the expected radiative transition pathways to create the luminescence bands B and L. E_A is the activation energy required to overcome entrapment in the meta-stable CB band, which minimum is located E_B above the CB edge. E_L describes the highest energy state above the VB edge involved to create the triple-sub-band feature of band L. The path through $^4T_{1g}(^4P)$ is depicted for illustrative purposes. (c) Depiction of a 2 : 1 LDH lattice with perfect ordering of Mg^{2+} and Al^{3+} ions in the lattice replaced with (1) a Co^{3+} ion (nearest neighbours Mg or Co cations) and (2) a Co^{2+} ion (nearest neighbours Al, Mg or Co cations). The likelihood of a Co-nearest-neighbour increases with Co-content.

two Co ions have different radii and cause small, local distortions in the lattice and decreases in local layer charge density. This effect is most pronounced for the replacement of Mg^{2+} with Co^{2+}, as high spin Co^{2+} is 0.25 Å larger in radius (0.745 Å) than Mg^{2+}.[35] Similarly, low spin Co^{3+} has a slightly larger ionic radius (0.545 Å) than Al^{3+} (0.535 Å)[35] and would thus also cause a slight decrease in local layer charge density and distortion of the lattice. A lower layer charge density around the Co (creating a charge deficient island) would preferentially attract excited electrons and may be just sufficient to temporarily (loosely) trap them. If this entrapment is not too deep, thermal activation could reverse the trapping and allow the excited electrons to relax to the CB edge before recombining with a hole in the VB—yielding the luminescence of band L (similar to the observation of increased luminescence with a filling of defect states in air[36]). This mechanism of exciton trapping frequently leads to emission at energies subceeding the bandgap,[6] as can be observed for MgCoAl-15.

The process of de-entrapment may be aided by polaron formation—a coupling of electrons and phonons—and, similarly, a coupling of the excitons and phonons. Polaron formation would require for there to be strong electron–phonon coupling.[6] MgCoAl-15 shows particularly strong lattice vibrations through anharmonic vibrational behaviour in the infrared region around 0.85 eV (step change in absorption strength not seen in the other materials in Fig. 1(a)). The region houses the first overtones of the MO–H stretching, H_2O stretching, H-bonding and H_2O–CO_3^{2-} bridging vibrations.[10] Thus, polaron formation may be especially strong for this material, aiding in overcoming the required activation energy to reach the band edge.

While an overcoming of exciton entrapment in the meta-stable band explains the general presence of band L, it does not give reason for its sub-band fine-structure. 81% of the luminescence of band L occurs at energies lower than the bandgap (at 298 K), representing a large fraction of the overall luminescence of band L. We propose that the sub-band-nature of band L (L_1, L_2 and L_3) maybe a result of a recombination with a hole temporarily located on the interlayer carbonate cation, leading to the emission of photons with an energy matching the difference between the CB edge and the carbonate vibrational levels.

At 83 K $\Delta(L_1 - L_2)$ = 0.17 eV and $\Delta(L_1 - L_3)$ = 0.33 eV. This matches perfectly with the carbonate vibrational levels above the VB edge with an energy of 0.17 eV for the fundamental $\nu_{3a,b}CO_3^{2-}$ vibration[10] and 0.34 eV for the $\nu_3CO_3^{2-}$ combination vibration.[10] These levels are indicated in Fig. 2(b).

An alternative explanation for the presence of band L_3 could be the involvement of a deactivation pathway through the Laporte forbidden d–d transition $^4T_{1g}(^4P)$, which is of slightly higher energy than the L_3 peak at 83 K. Use of such a pathway would indicate that an excited electron generated through a oxygen-to-metal transition relaxes by making use of a Laporte-forbidden transition, however. Evidence of such behaviour has been observed in Fe-modified bulk ZnSe polycrystals in the past.[37] In LDHs, behaviour which could support such a mechanism has been observed for NiAl-LDH[38] and CoAl-LDH[39] through excitation of the absorption band in the region of the d–d transition. However, further study is required to ascertain the involvement of the d–d transition instead of, for example, a defect state in the band tail.

We thus believe that the involvement of the carbonate ion is the more likely cause of the triple-band structure of band L. Its theoretical involvement in the recombination mechanism[10] has been strengthened by experimental results concerning an enhanced photocatalytic activity for carbonate-intercalated LDHs[40] but may only be viable in $M^{2+}M^{3+}$ LDHs, since for LiAl-LDH, carbonate presence in the interlayer caused a depression of luminescence.[30]

In summary, the recombination is believed to occur above the band edge through a meta-stable band causing the broad-emission-band B, from the CB edge through thermal activation to overcome the bottleneck of entrapment at Co island sites causing the strong-emission-band L, and below the band edge by recombination with a hole located at the carbonate anion. The bottleneck to non-radiative relaxation within the CB to the band edge points to an inhomogeneity in the density of states as an origin. An activated process may result in a delay in luminescence, which has been observed in other materials[1] and has interesting application potentials in LEDs,[2,3] scintillators[4] and thermal sensing.[5]

The results presented in this communication show that, besides inorganic materials such as perovskites, LDHs too are capable of producing rare, thermally activated luminescence. The strong increase in luminescence intensity at 298 K, little deviation in peak position and emission of blue-to-purple light make these materials an interesting choice for potential application in thermally stable blue-to-purple-light emitters. Time-resolved absorption and luminescence spectra, and the determination of electron spin are expected to further clarify the excitation and recombination mechanisms occurring within the LDH. The results of such studies may be supplemented by application in LEDs to ascertain whether the bulk properties of MgCoAl-15 can be used to create LEDs with attractive and abundant long-lived blue-to-purple light emission at room temperature. Further tuning of the thermal-activation behaviour and potential modulation of the luminescence bandwidth may render these materials an alternative in *e.g.* low cost LED applications. Study of structural effects on LDH luminescence may provide additional insight to other LDHs showing thermally activated luminescence behaviour.

Author contributions

The idea for this manuscript was developed by BRG and ER. Synthesis, experimental work and initial draft writing were conducted by BRG. BRG and ER analysed and interpreted the data together and prepared the final version of the manuscript. BRG, ER, AL and FJWJL contributed to review of the manuscript. All authors have given approval to the final version of the manuscript.

Conflicts of interest

There are no conflicts to declare.

Acknowledgements

The authors extend particular thanks to Prof. Reinhardt Botha (SA National Laser Centre) from the Department of Physics at the Nelson Mandela University, South Africa, and to Dr Evgenia Dmitrieva and Sandra Schiemenz from the Leibniz Institute for Solid State and Materials Research in Dresden, Germany, for their generosity and time to allow the use of their equipment to obtain luminescence spectra (RB) and absorption spectra (ED & SS). This work was funded by Techsparks (Pty) Ltd, the Technology and Human Resources for Industry Programme (THRIP) (Grant No.: THRIP/133/31/03/2016) through the National Research Foundation (NRF) South Africa, and the Technology and Innovation Agency (TIA) (2019 Seed Fund, A1C276). BRG would like to thank the L'Orèal-UNESCO Foundation for her PhD grant as part of the L'Orèal-UNESCO for Women in Science South Africa National Young Talents Award encouraging and making possible her independent work, as well as the University of Pretoria for her doctoral scholarship and the Leibniz-Institute for Polymer Research Dresden, e.V. for her visiting scientist stipend.

Notes and references

1 J. C. Sancho-García, *Nature*, 2022, **609**, 473–475.
2 D. Das, P. Gopikrishna, D. Barman, R. B. Yathirajula and P. K. Iyer, *Nano Convergence*, 2019, **6**, 1–28.
3 D. Barman, K. Narang, R. Gogoi, D. Barman and P. K. Iyer, *J. Mater. Chem. C*, 2022, **10**, 8536–8583.
4 F. Zhang, Y. Zhou, Z. Chen, M. Wang, Z. Ma, X. Chen, M. Jia, D. Wu, J. Xiao, X. Li, Y. Zhang, Z. Shi and C. Shan, *Adv. Mater.*, 2022, **34**, 2204801.
5 H. Zhang, J. Yao, K. Zhou, Y. Yang and H. Fu, *Chem. Mater.*, 2022, **34**, 1854–1861.
6 I. Pelant and J. Valenta, *Luminescence Spectroscopy of Semiconductors*, Oxford University Press, Oxford, 2012, p. 542.
7 S. Liu, B. Yang, J. Chen, D. Wei, D. Zheng, Q. Kong, W. Deng and K. Han, *Angew. Chem., Int. Ed.*, 2020, **59**, 21925–21929.
8 C. Forano, T. Hibino, F. Leroux and C. Taviot-Guého, *Dev. Clay Sci.*, 2006, **1**, 1021–1095.
9 V. Rives, *Layered Double Hydroxides: Present and Future*, Nova Science Publishers, Inc., New York, 2001.
10 B. R. Gevers, E. Roduner and F. J. Labuschagné, *Mater. Adv.*, 2022, **3**, 962–977.
11 B. R. Gevers, *The effects of transition-metal modification on MgMAl-layered double hydroxides for use in photofunctional applications*, 2022.
12 Y. Wu, H. Wang, Y. Sun, T. Xiao, W. Tu, X. Yuan, G. Zeng, S. Li and J. W. Chew, *Appl. Catal., B*, 2018, **227**, 530–540.
13 Z. Cai, X. Bu, P. Wang, J. C. Ho, J. Yang and X. Wang, *J. Mater. Chem. A*, 2019, **7**, 5069–5089.
14 Q. Chen, Y. Yu, J. Li, H. Nan, S. Luo, C. Jia, P. Deng, S. Zhong and X. Tian, *ChemElectroChem*, 2022, **9**, e202101387.
15 S. Naseem, B. Gevers, F. Labuschagné and A. Leuteritz, *Materials*, 2020, **13**, 4384.
16 B. Schwenzer, J. R. Neilson, K. Sivula, C. Woo, J. M. Fréchet and D. E. Morse, *Thin Solid Films*, 2009, **517**, 5722–5727.
17 X. Long, Z. Wang, S. Xiao, Y. An and S. Yang, *Mater. Today*, 2016, **19**, 213–226.
18 M. Shao, R. Zhang, Z. Li, M. Wei, D. G. Evans and X. Duan, *Chem. Commun.*, 2015, **51**, 15880–15893.

19 C. Coluccini, I. Sporer, A. Leuteritz, I. Kuehnert and D.-Y. Wang, *Nanomater. Energy*, 2014, **3**, 177–191.
20 W. Shi, M. Wei, D. G. Evans and X. Duan, *J. Mater. Chem.*, 2010, **20**, 3901–3909.
21 G. Prestopino, G. Arrabito, A. Generosi, A. Mattoccia, B. Paci, G. Perez, G. Verona-Rinati and P. G. Medaglia, *Sci. Rep.*, 2019, **9**, 1–12.
22 P. Ma, Y. Hou, Z. Chen, J. Su, L. Li, N. Liu, Z. Zhang, X. Jiang, F. Long, Y. Ma and Y. Gao, *Chem. Eng. J.*, 2021, **425**, 130471.
23 R. Liang, S. Xu, D. Yan, W. Shi, R. Tian, H. Yan, M. Wei, D. G. Evans and X. Duan, *Adv. Funct. Mater.*, 2012, **22**, 4940–4948.
24 D. Yan, J. Lu, M. Wei, S. Qin, L. Chen, S. Zhang, D. G. Evans and X. Duan, *Adv. Funct. Mater.*, 2011, **21**, 2497–2505.
25 W. Liu, R. Liang and Y. Lin, *Nanoscale*, 2020, **12**, 7888–7894.
26 Y. Liu, W. Sun, J. Xiao, Y. Fu, B. Shi and C. Lü, *Appl. Clay Sci.*, 2022, **229**, 106662.
27 B. R. Gevers, S. Naseem, A. Leuteritz and F. J. Labuschagné, *RSC Adv.*, 2019, **9**, 28262–28275.
28 E. S. Zhitova, S. V. Krivovichev, V. N. Yakovenchuk, G. Y. Ivanyuk, Y. A. Pakhomovsky and J. A. Mikhailova, *Mineral. Mag.*, 2018, **82**, 329–346.
29 R. Burns, *Mineralogical Applications of Crystal Field Theory*, Cambridge University Press, 2005.
30 S. H. Huang, S. J. Liu and J. Y. Uan, *J. Mater. Chem. C*, 2019, **7**, 11191–11206.
31 R. Gao, D. Yan and X. Duan, *Cell Rep. Phys. Sci.*, 2021, **2**, 100536.
32 Y. Fu, F. Ning, S. Xu, H. An, M. Shao and M. Wei, *J. Mater. Chem. A*, 2016, **4**, 3907–3913.
33 J. Shi, S. Li, F. Wang, L. Gao, Y. Li, X. Zhang and J. Lu, *J. Alloys Compd.*, 2018, **769**, 611–619.
34 Z. Zhang, G. Chen and K. Xu, *Ind. Eng. Chem. Res.*, 2013, **52**, 11045–11049.
35 R. D. Shannon, *Acta Crystallogr., Sect. A: Cryst. Phys., Diffr., Theor. Gen. Crystallogr.*, 1976, **32**, 751–767.
36 A. W. Cohn, A. M. Schimpf, C. E. Gunthardt and D. R. Gamelin, *Nano Lett.*, 2013, **13**, 1810–1815.
37 K. A. Jeong, S. K. Lee and N. Myoung, *Opt. Mater. Express*, 2019, **9**, 2964.
38 S. Intachai, T. Nakato and N. Khaorapapong, *Appl. Clay Sci.*, 2021, **201**, 105927.
39 Y. Qiu, B. Lin, F. Jia, Y. Chen, B. Gao and P. Liu, *Mater. Res. Bull.*, 2015, **72**, 235–240.
40 L. Mohapatra and K. Parida, *J. Mater. Chem. A*, 2016, **4**, 10744–10766.

